The Canadian Mineralogist
Vol. 60, pp. 361-368 (2022)
DOI: 10.3749/canmin.2100054

THE REDEFINITION OF GUNTERITE, $Na_4Ca[V_{10}O_{28}]·20H_2O$

ANTHONY R. KAMPF[§]

Mineral Sciences Department, Natural History Museum of Los Angeles County, 900 Exposition Boulevard, Los Angeles, California 90007, USA

MARK A. COOPER AND FRANK C. HAWTHORNE

Department of Earth Sciences, University of Manitoba, 125 Dysart Road, Winnipeg, Manitoba R3T 2N2, Canada

JOHN M. HUGHES

Department of Geology, University of Vermont, 180 Colchester Ave., Burlington, Vermont 05405, USA

BARBARA P. NASH

Department of Geology and Geophysics, University of Utah, 115 S 1460 E, Salt Lake City, Utah 84112, USA

PAUL M. ADAMS

Mineral Sciences Department, Natural History Museum of Los Angeles County, 900 Exposition Boulevard, Los Angeles, California 90007, USA

ABSTRACT

Gunterite was originally assigned the ideal formula $Na_4[H_2V_{10}O_{28}]·22H_2O$. More detailed bond-valence analysis brought into question the presence of a protonated decavanadate anion, which led to the reexamination of the mineral. Infrared spectroscopy confirmed the absence of NH_4. Reinterpretation of the original crystal structure data and new electron-probe microanalyses support the redefinition of gunterite as having the ideal formula $Na_4Ca[V_{10}O_{28}]·20H_2O$. This redefinition has been approved by the Commission on New Minerals, Nomenclature and Classification of the International Mineralogical Association.

Keywords: gunterite, redefinition, crystal structure, decavanadate, pascoite family.

INTRODUCTION

The original description of gunterite from the West Sunday mine, San Miguel County, Colorado, USA (Kampf *et al*. 2011) reported the ideal formula of the species as $Na_4(H_2O)_{16}(H_2V_{10}O_{28})·6H_2O$ (or more simply $Na_4[H_2V_{10}O_{28}]·22H_2O$), indicating the decavanadate isopolyanion to be doubly protonated. That formula was based upon a structure determination that provided two interstitial cation sites corresponding to 4 *apfu*. One of these sites was split into two partially occupied sites separated by 0.76 Å, and this split site refined to a total occupancy of $Ca_{0.55}Na_{0.45}$. The excess charge from the heterovalent Ca ↔ Na substitution was presumed to be balanced by deprotonation of the decavanadate group, leading to the formula $(Na_{4–x}Ca_x)[H_{2–x}V_{10}O_{28}]·22H_2O$ and, because Na > Ca, the ideal formula above with only Na was proposed.

A very large number of decavanadate phases have been synthesized, and some of these have been reported to contain protonated decavanadate polyanions. Unfortunately, in most cases, structure determination failed to locate the H atoms on the protonated decavanadate polyanions. Cooper *et al*. (2019) surveyed 17 well-characterized structures of synthetic

---

[§] *Corresponding author e-mail address*: akampf@nhm.org

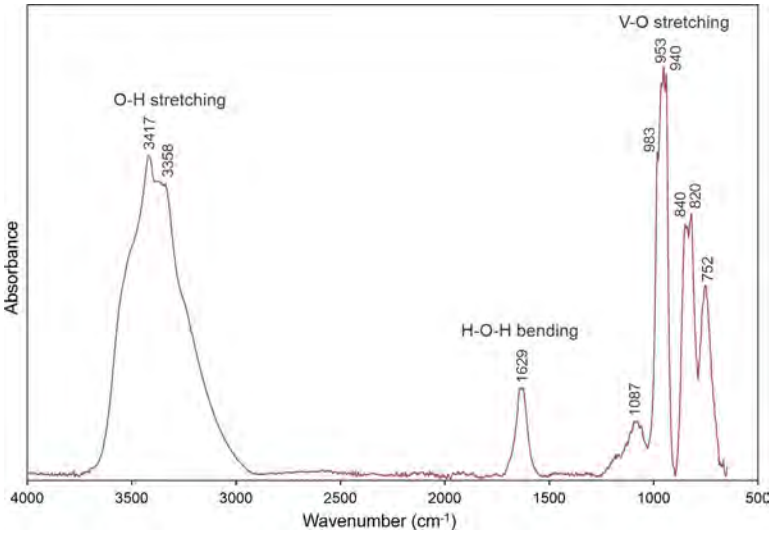

FIG. 1. FTIR spectrum of gunterite.

phases containing protonated decavanadate polyanions and developed a bond-valence approach for predicting which of the O atoms on the surface of the decavanadate polyanions are protonated. They calculated partial bond-valence sums at the decavanadate polyanions resulting from the V–O interactions alone ($s\ \Sigma_{OV}$) and found that non-protonated O atoms on the exterior of the decavanadate polyanion have $s\ \Sigma_{OV}$ values from ~1.7 to 2.0 *vu*, whereas protonated O atoms have significantly lower $s\ \Sigma_{OV}$ values, from ~1.2 to 1.5 *vu*.

Based upon this approach, Cooper *et al*. (2019) surmised that rakovanite, originally described as containing a triply protonated decavanadate polyanion and having the ideal formula $Na_3[H_3V_{10}O_{28}]\cdot15H_2O$, actually contained a non-protonated decavanadate polyanion. Rakovanite was subsequently found to contain three NH_4^+ cations *pfu*, which had been previously misidentified as H_2O, and it was redefined by Kampf *et al*. (2021) with the formula $(NH_4)_3Na_3[V_{10}O_{28}]\cdot12H_2O$. Cooper *et al*. (2019) could not conclusively confirm protonated exterior O sites on the decavanadate polyanion in gunterite and recommended that gunterite be reexamined. Herein, we report on the reevaluation of the structure refinement and electron-probe microanalyses (EPMA) for gunterite, which support the revision of its ideal formula to $Na_4Ca[V_{10}O_{28}]\cdot20H_2O$. This revision has been approved by the Commission on New Minerals, Nomenclature and Classification of the International Mineralogical Association (Miyawaki *et al*. 2021).

INFRARED SPECTROSCOPY

In order to rule out the presence of significant NH_4^+ in gunterite, Fourier transform infrared (FTIR) spectroscopy was done using a Thermo Scientific iS50 FTIR spectrometer equipped with a Continuμm microscope. The sample was analyzed in transmission mode with a diamond compression cell at 4 cm^{-1} resolution through one diamond window. The FTIR spectra for gunterite crystals from cotype specimen 63507 recorded from 4000 to 650 cm^{-1} is shown in Figure 1. Most notably, the distinctive band at approximately 1400 cm^{-1} assignable to NH_4^+ deformation (Chukanov & Chervonnyi 2016) is absent in the spectrum, so the absence of a significant amount of NH_4^+ in gunterite is confirmed.

CRYSTAL STRUCTURE

Based on the original structure determination for gunterite (conducted using a crystal from cotype specimen #63506), we calculated partial bond-valence sums for the O atoms on the exterior of the decavanadate polyanion resulting from the V–O interactions alone ($s\ \Sigma_{OV}$) and found $s\ \Sigma_{OV}$ values from ~1.75 to 1.90 *vu*, thus confirming the decavanadate polyanion to be unprotonated. In reexamining the interstitial complex, we note that the fully occupied OW8 site cannot be an O site because of its close proximity to six fully occupied O sites [O2, OW2, OW4 (×2), and OW6 (×2)] at distances ranging from 2.36 to 2.48 Å. Furthermore, these surrounding O sites are arranged such that they form a slightly distorted octahedral arrangement around the

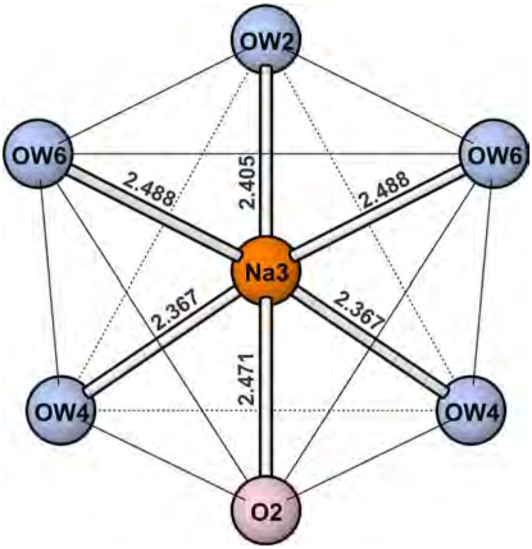

FIG. 2. The octahedral coordination of the newly assigned half-occupied Na3 site.

OW8 site. In a new refinement based on the original structure data, we assigned Na to the original OW8 site (now labeled Na3) and noted it to be approximately half-occupied. The octahedral coordination, shown in Figure 2, is typical for Na; <Na3–O> = 2.431 Å and the bond-valence sum received by Na at this site is 1.04 *vu* (based on bond-valence parameters from Gagné & Hawthorne 2015). The Na3 site is 2.74 Å from the Ca2 site; both Na3 and Ca2 are 4*i* sites, and both are approximately 1/2 occupied, so they show dependent occupancy in order to avoid close approach. Additionally, in our new refinement, we have opted to split the OW3 and OW5 sites, as their local occupancies and local distances to Na2/Ca2 support two locally coupled environments. Due to the large amount of disorder observed for the interstitial constituents, we have not attempted H atom modeling in our new structure refinement. The original data collection details and the new refinement details are given in Table 1. Atom coordinates, displacement parameters, and site occupancies are given in Table 2. Note that the occupancy of the Na3 site refined to 0.332; however, we base the revised formula on an ideal occupancy of 0.5 for this site and ideal occupancies of 0.5 for the Na2 and Ca2 sites.

TABLE 1. DATA COLLECTION AND STRUCTURE REFINEMENT DETAILS FOR GUNTERITE

Diffractometer	Rigaku R-Axis Rapid II
X-ray radiation / power	Mo$K\alpha$ (λ = 0.71075 Å) / 50 kV, 40 mA
Temperature	298(2) K
Structural Formula	$Na_{3.75}Ca_{0.91}[V_{10}O_{28}]\cdot 20H_2O$ (with unlocated H included)
Space group	$C2/m$
Unit-cell dimensions	a = 19.848(2) Å
	b = 10.1889(11) Å
	c = 13.1184(15) Å
	β = 130.187(9)°
Z	2
V	2026.6(5) Å^3
Density (for above formula)	2.361 g/cm^3
Absorption coefficient	2.487 mm^{-1}
F(000)	1427.1
Crystal size	250 × 150 × 30 μm
θ range	3.11 to 20.80°
Index ranges	$-19 \le h \le 19$, $-10 \le k \le 10$, $-13 \le l \le 13$
Reflections collected / unique	8230 / 1130 [R_{int} = 0.090]
Reflections with $I_o > 2\sigma I$	931
Completeness to θ = 20.80°	99.5%
Refinement method	Full-matrix least-squares on F^2
Parameters/restraints	172/0
GoF	1.040
Final R indices [$I_o > 2\sigma I$]	R_1 = 0.0616, wR_2 = 0.1652
R indices (all data)	R_1 = 0.0705, wR_2 = 0.1782
Largest diff. peak / hole	+1.03 / –0.62 e/A^3

Notes: $R_{int} = \Sigma|F_o^2 - F_o^2(\text{mean})|/\Sigma[F_o^2]$. GoF = $S = \{\Sigma[w(F_o^2 - F_c^2)^2]/(n-p)\}^{1/2}$. $R_1 = \Sigma||F_o| - |F_c||/\Sigma|F_o|$. $wR_2 = \{\Sigma[w(F_o^2 - F_c^2)^2]/\Sigma[w(F_o^2)^2]\}^{1/2}$. $w = 1/[\sigma^2(F_o^2) + (aP)^2 + bP]$ where a is 0.1332, b is 0 and P is $[2F_c^2 + \text{Max}(F_o^2,0)]/3$.

TABLE 2. ATOM COORDINATES, DISPLACEMENT PARAMETERS (Å^2), AND SITE OCCUPANCIES IN GUNTERITE

	x/*a*	*y*/*b*	*z*/*c*	U_{eq}	Occupancy	U^{11}	U^{22}	U^{33}	U^{23}	U^{13}	U^{12}
Na1	0.3135(3)	0.5	0.0406(6)	0.0669(15)	1	0.058(3)	0.049(3)	0.099(4)	0	0.052(3)	0
Na2	0.6284(19)	0.5	0.352(3)	0.062(4)	0.54(3)	0.067(11)	0.040(6)	0.110(15)	0	0.071(12)	0
Ca2	0.6712(8)	0.5	0.4163(13)	0.042(3)	0.46(3)	0.029(6)	0.038(3)	0.067(7)	0	0.035(6)	0
Na3	0.7609(9)	0.5	0.6873(15)	0.053(6)	0.332(17)	0.065(11)	0.044(9)	0.080(12)	0	0.059(10)	0
V1	0	0.33852(16)	0.5	0.0338(7)	1	0.0301(12)	0.0287(12)	0.0484(15)	0	0.0280(11)	0
V2	0.93436(11)	0.5	0.62856(19)	0.0374(7)	1	0.0307(12)	0.0367(12)	0.0518(15)	0	0.0298(11)	0
V3	0.82095(11)	0.5	0.32245(19)	0.0371(7)	1	0.0286(12)	0.0369(12)	0.0509(14)	0	0.0279(11)	0
V4	0.88651(8)	0.34893(12)	0.19498(14)	0.0397(7)	1	0.0359(10)	0.0345(10)	0.0507(12)	–0.0024(6)	0.0289(9)	–0.0008(6)
O1	0.7339(5)	0.5	0.3092(8)	0.044(2)	1	0.031(4)	0.049(4)	0.051(5)	0	0.027(4)	0
O2	0.8446(5)	0.5	0.6073(8)	0.048(2)	1	0.043(5)	0.053(5)	0.063(5)	0	0.042(5)	0
O3	0.9492(3)	0.2376(5)	0.3643(5)	0.0368(14)	1	0.034(3)	0.033(3)	0.052(4)	–0.003(2)	0.031(3)	–0.002(2)
O4	0.8480(5)	0.5	0.0942(7)	0.0404(19)	1	0.042(4)	0.028(4)	0.050(5)	0	0.029(4)	0
O5	0.0502(4)	0.5	0.6333(7)	0.034(2)	1	0.033(4)	0.032(4)	0.046(5)	0	0.029(4)	0
O6	0.8976(3)	0.6214(5)	0.4811(5)	0.0340(14)	1	0.033(3)	0.026(3)	0.052(4)	–0.002(2)	0.032(3)	–0.001(2)
O7	0.9995(3)	0.6317(5)	0.7485(5)	0.0406(14)	1	0.037(3)	0.035(3)	0.054(4)	–0.006(2)	0.031(3)	–0.003(2)
O8	0.8491(3)	0.2305(5)	0.0896(5)	0.0478(15)	1	0.046(4)	0.037(3)	0.060(4)	–0.012(2)	0.034(3)	–0.008(2)
O9	0.7992(3)	0.3690(4)	0.2107(5)	0.0370(14)	1	0.035(3)	0.035(3)	0.047(3)	–0.004(2)	0.029(3)	–0.003(2)
OW1	0.4165(6)	0.5	0.0049(10)	0.073(3)	1	0.063(6)	0.064(5)	0.095(7)	0	0.052(6)	0
OW2	0.3232(7)	0.5	0.2395(11)	0.097(3)	1	0.112(9)	0.092(7)	0.102(9)	0	0.076(8)	0
OW3	0.5819(12)	0.6626(11)	0.240(2)	0.054(2)	0.48(2)						
OW3′	0.5508(11)	0.6694(11)	0.173(2)	0.054(2)	0.52(2)						
OW4	0.7004(5)	0.6770(6)	0.5347(8)	0.086(2)	1	0.074(5)	0.065(4)	0.131(7)	0.008(4)	0.072(5)	0.019(3)
OW5	0.5446(13)	0.5	0.411(2)	0.073(4)	0.558(16)						
OW5′	0.4955(16)	0.5	0.314(3)	0.073(4)	0.442(16)						
OW6	0.6691(5)	0.1972(7)	0.1672(8)	0.090(2)	1	0.099(6)	0.087(5)	0.106(6)	0.007(4)	0.075(5)	0.003(4)
OW7	0.5744(13)	0	0.0189(15)	0.185(8)	1	0.38(3)	0.075(8)	0.148(13)	0	0.195(17)	0

TABLE 3. INTERATOMIC DISTANCES (*d* IN Å) AND BOND VALENCES (*v* IN VALENCE UNITS) IN THE INTERSTITIAL COMPLEX

	d	*v*		*d*	*v*
Na1–O4	2.467(8)	0.16	Ca2–O1	2.404(13)	0.30
Na1–O8 (×2)	2.417(5)	0.18	Ca2–O2	2.645(15)	0.16
Na1–O9 (×2)	2.852(7)	0.06	Ca2–OW3 (×2)	2.44(2)	0.27
Na1–OW1	2.373(10)	0.20	Ca2–OW4 (×2)	2.200(10)	0.49
Na1–OW2	2.490(12)	0.15	Ca2–OW5′	2.82(2)	0.11
Na1–OW5′	*3.03(3)*	[*0.04*]	BVS		2.09
BVS		0.99 [*1.03*]			
			Na3–O2	2.471(14)	0.16
Na2–O1	2.491(15)	0.15	Na3–OW2	2.405(16)	0.18
Na2–OW3′ (×2)	2.49(3)	0.15	Na3–OW4 (×2)	2.367(12)	0.20
Na2–OW4 (×2)	2.57(2)	0.12	Na3–OW6 (×2)	2.488(11)	0.15
Na2–OW5	2.25(2)	0.27	*Na3–OW7*	*3.05(2)*	[*0.04*]
BVS		0.96	BVS		1.04 [*1.08*]
Cation–cation and anion–anion distances					
Na2–Ca2	0.72(2)		OW3–OW3′	0.683(15)	
Ca2–Na3	2.764(19)		OW5–OW5′	0.99(2)	
Na2–Na3	3.37(3)				

Bond-valence parameters are from Gagné & Hawthorne (2015).
Note that weak longer bonds are shown in italics.

In our detailed analysis of the interstitial complex in the gunterite structure, we have included the longer Na1–OW5′ (3.03 Å) and Na3–OW7 (3.05 Å) contacts as weak longer bonds; this is based mainly on the 'splayed' character to the coordinations (*i.e.*, for Na3 the 11 internal φ–Na3–φ angles for octahedral coordination range from 75.8 to 103.5°, whereas OW6–Na3–OW6 opens up to 107.8° to accommodate the approach by OW7). The Na1–OW5′ bond occurs only ~50% of the time (*i.e.*, when nearby OW5′ is occupied) and OW7 receives only weak bonding from Na ~50% of the time (*i.e.*, when Na3 is occupied by Na). Regarding the split H_2O groups OW3/OW3′ and OW5/OW5′, Ca2 bonds to OW3 and OW5′, whereas Na2 bonds to OW3′ and OW5; this is supported by similar refined occupancies within each grouping as well as the resulting conformable bond-valence sums at the Na2 and Ca2 sites (Table 3). The combined site occupancies, interatomic distances, and bond valences support two distinct arrangements of the interstitial components: ~50% Na2–OW3′–OW5–Na3 and ~50% Ca2–OW3–OW5′–□. These two arrangements lead to interstitial compositions $Na_6(H_2O)_{20}$ and $Na_2Ca_2(H_2O)_{20}$. We note that the refined structure and chemical analysis for gunterite collectively support an interstitial composition near the midpoint between these two compositions, *i.e.*, $Na_4Ca(H_2O)_{20}$. Interestingly, kokinosite has an ordered structure with formula $Na_2Ca_2[V_{10}O_{28}]\cdot 24H_2O$, and therefore has the same interstitial cation character as one of the local arrangements inferred for the disordered structure of gunterite. The interstitial complex with all disordered (partly occupied) constituents and two local configurations is shown in Figure 3. The complete structure is shown in Figure 4.

CHEMICAL COMPOSITION

The electron-probe microanalyses (EPMA) were collected at the University of Utah using a Cameca SX-50 electron microprobe with four wavelength-dispersive spectrometers. Analytical conditions were 15 keV accelerating voltage, 10 nA beam current, and a nominal beam diameter of 10 μm, although a larger diameter of 15 μm was occasionally used on larger fragments. Count times were 10 s for each element. Raw X-ray intensities were corrected for matrix effects with a ϕρ(z) algorithm (Pouchou & Pichoir 1991).

Gunterite was very challenging to analyze, particularly because of the dehydration of crystals under vacuum and the concomitant degradation of the polished crystal surfaces. Na_2O values were particularly problematic, showing a high degree of variability. The nine analyses that were originally reported were thought to be the most reliable. In retrospect, our selection of EPMA compositions was clearly biased by our original interpretation of the crystal structure. In light of our reassessment of the crystal structure, it seems likely that the analyses reported suffered from Na loss during analysis, which was not accounted for. Herein (Table 4), we report five analyses, which we believe are the most representative of the true

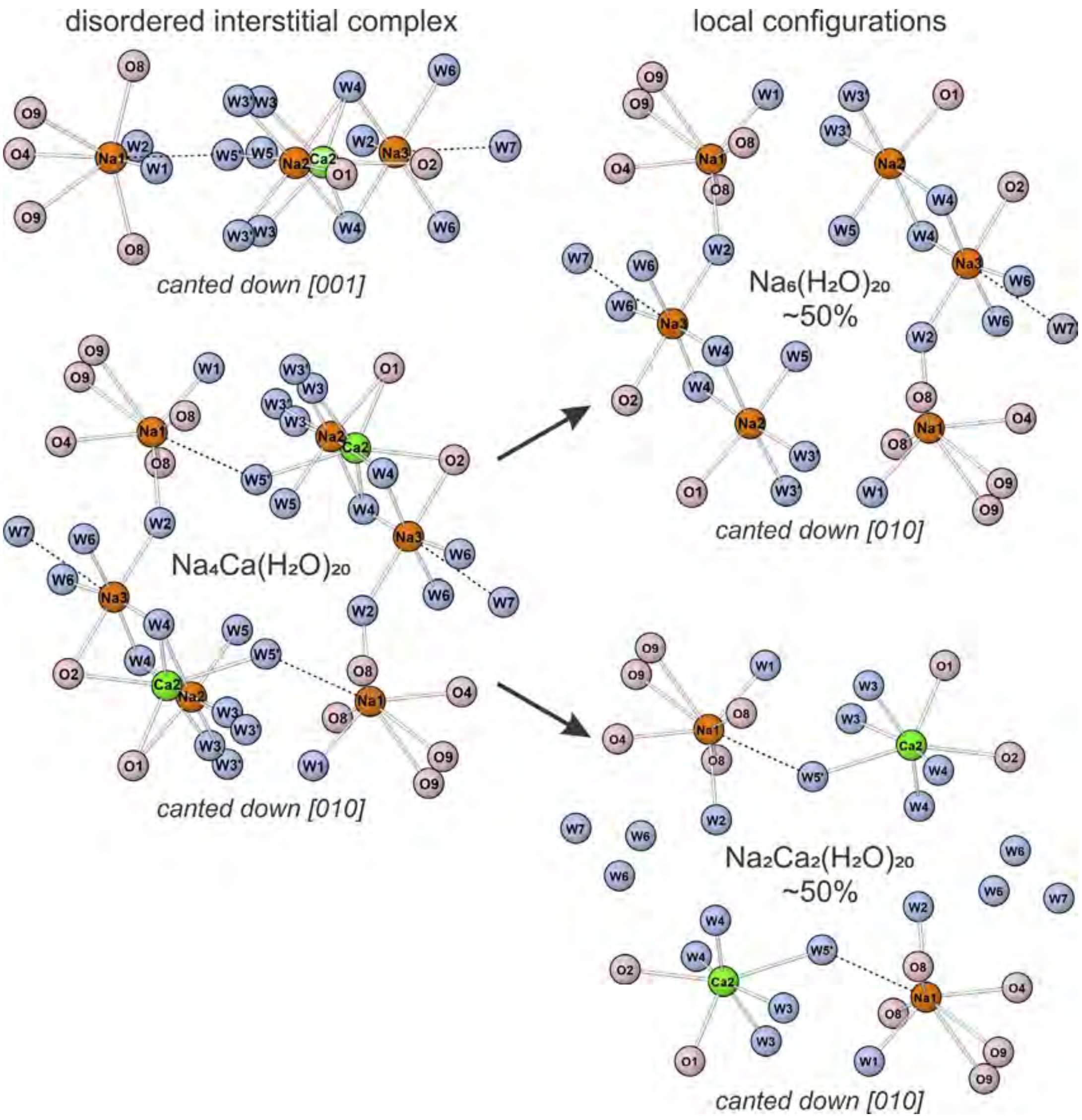

FIG. 3. The interstitial complex in gunterite. Note that decavanadate O atoms are pink and interstitial H_2O O atoms (with W rather than OW labels) are blue. Weak longer bonds are shown as dashed lines.

composition of gunterite. It is also worth noting that N was specifically sought by EPMA, but none was detected.

Note that during vacuum deposition of the conductive carbon coat required for the EPMA, gunterite was subjected to an ultimate vacuum of 2×10^{-5} torr for approximately 5 min. This clearly resulted in the loss of much of the weakly held H_2O. The very large H_2O loss resulted in much higher concentrations for the remaining constituents than are to be expected for the fully hydrated phase; therefore, the other analyzed constituents have been normalized to provide a total of 100% when combined with the calculated H_2O content.

The empirical formula based on 10 V and 48 O *apfu* is $(Na_{4.28}Ca_{0.88})_{\Sigma 5.16}[V_{10}O_{28}]\cdot 20H_2O$ (–0.04 H for charge balance) and the ideal formula is $Na_4Ca[V_{10}O_{28}]\cdot 20H_2O$, which requires Na_2O 8.55, CaO 3.87, V_2O_5 62.73, H_2O 24.85, total 100.00 wt.%. It can be noted that the Gladstone-Dale compatibility $1 - (K_p/K_c) = -0.016$ for both the empirical and ideal formulas, in the range of superior compatibility.

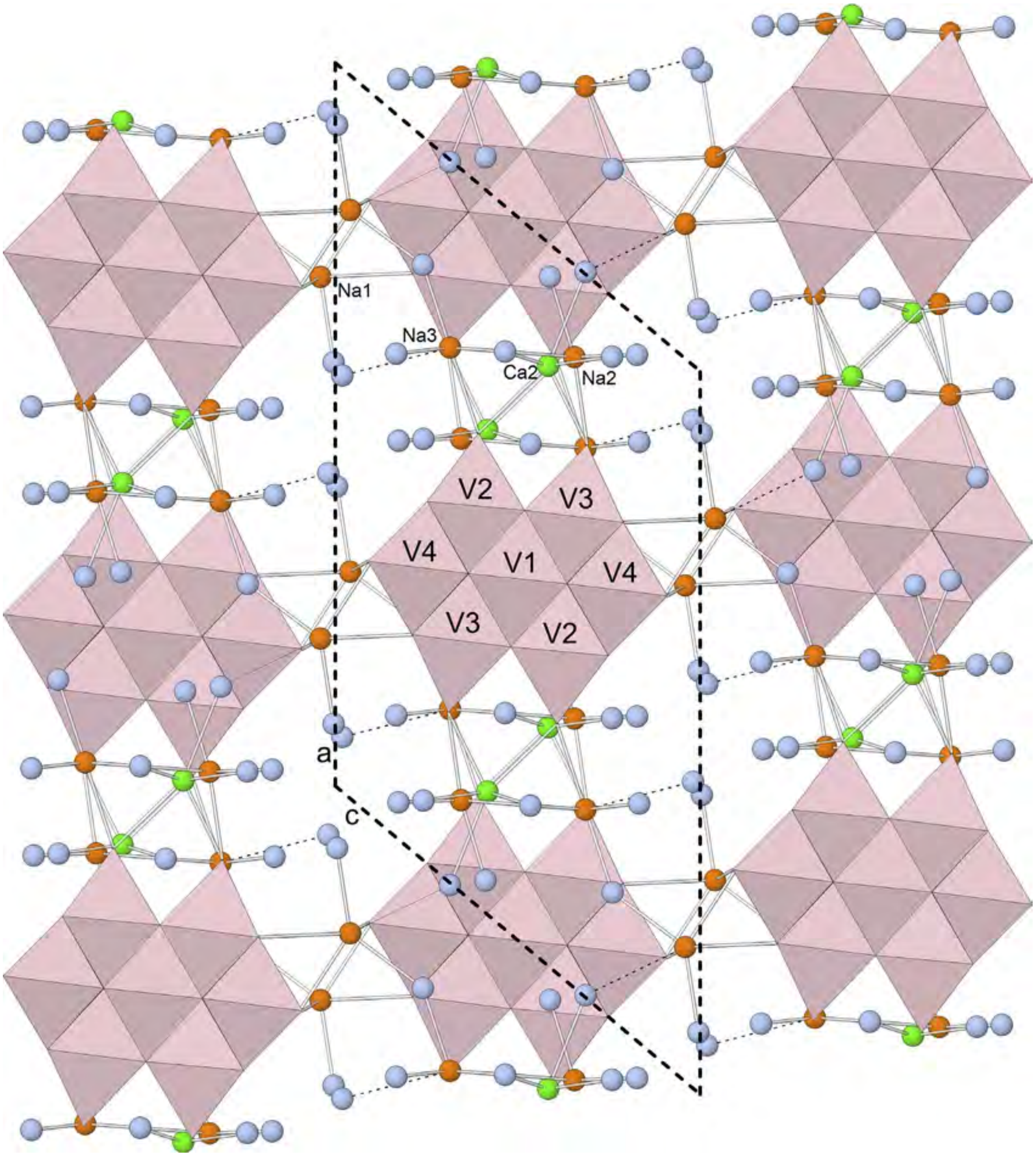

FIG. 4. The crystal structure of gunterite viewed down [010]. The unit-cell outline is shown with dashed lines.

TABLE 4. ANALYTICAL DATA IN wt.% FOR GUNTERITE

Constituent	Mean	Range	S.D.	Standard	Normalized
Na_2O	10.37	9.36–11.72	1.18	albite	9.14
CaO	3.85	3.45–4.76	0.53	diopside	3.39
V_2O_5	71.09	69.50–72.39	1.21	V metal	62.66
H_2O					24.80*
Total					99.99

* Based upon the crystal structure with V = 10 and O = 48 *apfu*.

CONCLUSION

The foregoing evidence clearly supports the redefinition of gunterite as an unprotonated decavanadate with the ideal formula $Na_4Ca[V_{10}O_{28}]\cdot 20H_2O$.

ACKNOWLEDGMENTS

The manuscript was improved by reviews from Travis Olds and Inna Lykova. The study was supported, in part, by the John Jago Trelawney Endowment to the Mineral Sciences Department of the Natural History Museum of Los Angeles County and by a Discovery Grant to FCH from the Natural Sciences and Engineering Council of Canada.

REFERENCES

CHUKANOV, N.V. & CHERVONNYI, A.D. (2016) *Infrared Spectroscopy of Minerals and Related Compounds*. Springer: Cham–Heidelberg– Dordrecht–New York–London.

COOPER, M.A., HAWTHORNE, F.C., KAMPF, A.R., & HUGHES, J.M. (2019) Identifying protonated decavandate polyanions. *Canadian Mineralogist* **56**, 245–253.

GAGNÉ, O.C. & HAWTHORNE, F.C. (2015) Comprehensive derivation of bond-valence parameters for ion pairs involving oxygen. *Acta Crystallographica* **B71**, 562–578.

KAMPF, A.R., HUGHES, J.M., MARTY, J., & NASH, B. (2011) Gunterite, $Na_4(H_2O)_{16}(H_2V_{10}O_{28})\cdot 6H_2O$, a new mineral with a doubly–protonated decavanadate polyanion: Crystal structure and descriptive mineralogy. *Canadian Mineralogist* **49**, 1243–1251.

KAMPF, A.R., HUGHES, J.M., COOPER, M.A., HAWTHORNE, F.C., NASH, B.P., OLDS, T.A., ADAMS, P.M., & MARTY, J. (2021) The pascoite family of minerals, including the redefinition of rakovanite. *Canadian Mineralogist* **59**, 771–779.

MIYAWAKI, R., HATERT, F., PASERO, M., & MILLS, S.J. (2021) Newsletter 61. *Mineralogical Magazine* **85**, 459–463.

POUCHOU, J.-L. & PICHOIR, F. (1991) Quantitative Analysis of Homogeneous or Stratified Microvolumes Applying the Model "PAP." *In* Electron Probe Quantitation. Springer US, Boston, MA, USA (31–75).

Received August 23, 2021. Revised manuscript accepted December 7, 2021.